Enantioselective amino acid interactions in solution

Natsuki Watanabe, Mitsuo Shoji, Koichi Miyagawa, Yuta Hori, Mauro Boero, Masayuki Umemura, Yasuteru Shigeta

ARTICLE

Enantioselective Amino Acid interactions in Solution

Natsuki Watanabe [a], Mitsuo Shoji [*b,c], Koichi Miyagawa [b], Yuta Hori [b], Mauro Boero [d], Masayuki Umemura [b] and Yasuteru Shigeta [b]

Received 00th January 20xx,
Accepted 00th January 20xx

DOI: 10.1039/x0xx00000x

Enantiomeric excesses (ee) of L-amino acids in meteorites are higher than 10% especially for isovaline (Iva). This suggests the existence of some kind of trigarring mechanisms responsible for the amplification of the ee from an initial small value. Here, we investigate the dimeric molecular interactions of alanine (Ala) and Iva in solution as an initial nucleation step of crystals at an accurate first-principles level. We find that the dimeric interaction of Iva is more chirality-dependent than that of Ala, thus providing a clear molecular level insight into the enantioselectivity of amino acids in solution.

1 Introduction

Amino acids are the fundamental constituents of proteins, and most of living organisms on Earth adopt exclusively the L-form of chiral amino acids, with the only exception of achiral glycine, although chemical syntheses *in vitro* have evidenced the production of an equal amount of L- and D-forms as a racemic mixture. This observation indicates that a chiral symmetry breaking must be at the basis of the chemical evolution process occurred before the emergence of life in the early stage of Earth. A captivating scenario is an extra-terrestrial origin, in which L-amino acids were provided by comets and meteorites to ancient Earth and that determined the origin of homochirality of amino acids on Earth. This theory is supported by detections of amino acids in the Murchison meteorite, fallen on Australia in 1969, and the enantiomeric excess (ee) of L-amino acids were discovered to above 10%.[1-3] For an initial creation of ee, photochemical reactions with circularly polarized light (CPL) were shown to be essential.[4] However, the ee values produced by CPL irradiation are much lower compared to the ee values of meteoritic amino acids.[5-7] Therefore, an amplification process should exist to justify these high ee values in meteorites. One clue is that the ee values of meteoritic amino acids are correlated to aqueous alteration on meteorite parent bodies.[8,9] However, the mechanism still remains controversial because of the scarcity of meteoritic samples and potential contributions from terrestrial contaminations.[10-13]

Concerning aqueous alteration, Viedma and coworkers have shown that the ee of amino acids can be amplificated through the generation of conglomerate crystals.[14,15] In conglomerate crystals, each enantiomer is separately crystalized, and in the early stage a small amount of ee can be amplificated to higher values. The typical amino acids prone to form conglomerate crystals are aspartic acid (Asp), glutamic acid (Glu) and isovaline (Iva). Conversely, most of the other amino acids such as alanine (Ala) do not form conglomerate crystals but racemic compounds.[16,17] In the crystallization processes, two different mechanisms are expected to occur. One is the enantioselectivity which determines the nature of the crystal, either racemic or conglomerate. The second one is the enantioenrichment which includes both chemical steps of crystal growth and isomerization. Enantioenrichment by sublimation has also been proposed as an alternative process to crystalization.[18-19] Aqueous environments in ice dusts and meteorite parent bodies promote mainly crystallization rather than sublimation. However, in cosmochemical regions in the absence of any atmospheric pressure, sublimation represents a viable reaction path.

In the present study, we focus on the enantioselectivity to realize a crystal phase, with particular emphasis on the dimerization of amino acids representing the initial nucleation of the crystallization process. Malar and coworkers investigated the stable conformations of L-Ala dimers in gas phase,[20] and reported that the most stable form is a face-to-face arrangement of their carboxy groups, in which the molecular chirality is not influenced. In crystals and solutions, however, amino acids take a zwitterion form, and their molecular interactions change as a result of a lack of interactions between their carboxylate anions.

Here, we have investigated the molecular mechanisms of dimerization of amino acids in the zwitterion form by resorting to accurate first-principles calculations within the density functional theory (DFT) framework. For this purpose, we developed a versatile conformational sampling algorithm to determine the most stable conformers of the amino acid dimers.

[a] Graduate School of Pure and Applied Sciences, University of Tsukuba, 1-1-1 Tennodai, Tsukuba, Ibaraki 305-8571, Japan.
[b] Center for Computational Sciences, University of Tsukuba, 1-1-1 Tennodai, Tsukuba, Ibaraki 305-8577, Japan.
E-mail: mshoji@ccs.tsukuba.ac.jp
[c] JST-PRESTO, 4-1-8 Honcho, Kawaguchi, Saitama 332-0012, Japan.
[d] University of Strasbourg, Institut de Physique et Chimie des Matériaux de Strasbourg, CNRS, UMR 7504, 23 rue du Loess, F-67034 France.
†Electronic Supplementary Information (ESI) available. See DOI: 10.1039/x0xx000x

We focused on homochiral and heterochiral dimers of each amino acid Ala and Iva. Hereafter their dimer models are referred to as Ala-Ala for the Ala dimer and Iva-Iva for the Iva dimer. Furthermore, we investigated hetero-dimers composed of Ala and Iva to account for the possibility of chiral propagation between different amino acids. These are referred to as Ala-Iva hetero-dimers.

2 Computational details

Our new sampling approach spans a broad conformational space and uses different theoretical levels to refine optimized structures and to avoid intrinsic shortcomings of each approach. The DFT-based electronic structure calculation method provides reliable optimized structures and relative energies, showing that the dimerization is the result of a subtle interplay between hydrogen bonds (H-bonds) and van der Waals (vdW) forces for intra- and inter-molecular interactions as well as interactions with a solvent.[21, 22] However, direct application of the DFT approach to thousands of conformers is a heavy computational workload and time consuming. To encompass this difficulty, we used three different theoretical levels, namely a molecular mechanics method (MM) for the initial structural refinement, semi-empirical molecular orbital method (SEMO) for a second refinement, and DFT for a final assessment of the stable structures. The specific search algorithm used to obtain all the conformers is the one developed by our group reported in a former publication[23] and termed random sampling (RS) method. In the following section, an extension to amino acid dimers is detailed. A flowchart of the computational procedure is shown in Fig. 1.

1. Determine a molecule to be calculated, e.g., amino acid dimer, and prepare a 3-dimentional simulation cell sufficiently large to host the molecule. In this simulation cell we then place all the atoms which compose the dimer in uniformly distributed random positions. At this point, molecules are not yet forming the typical amino acid structures.

2. As a second step, a geometrical optimization is performed within a force field (FF) MM approach. This gives shape to the amino acid. Our simple FF composed of three terms for bond, angle bending and van der Waals interactions, which are sufficient for the initial structural optimization. Other terms generally used in MM calculations for dihedral angle and electrostatic interaction are excluded, since they will be included at higher level methodologies used in the subsequent steps. Additional details are provided in the supporting information.

3. Steps 1 and 2 are then repeated for a number of times, (generally > 1,000) to generate a sufficiently large number of conformations.

4. Geometrical optimizations and total energy calculations of the dimers are then performed using SEMO. The PM7 method implemented in the MOPAC 2016 package was used.[24] The solvation effect of water was incorporated by conductor-like screening model (COSMO).

5. The conformations obtained in step 4 are then classified according to the molecular chirality. Dimers composed of the same enantiomers and different enantiomers are called LL and LD, respectively. Relative energies were calculated and classified into either LL or LD. The increment of the energy distributions was set to 1 kcal mol^{-1}. When a replication of more than five times appeared in the lowest energy conformation, we typically interpreted that as the most stable conformation, and we went to the next final refinement step. When replication in the lowest energy distribution were not sufficient, we repeated the steps 1-4 until the lower energy states were generated with sufficient statistics.

6. For each LL and LD, we took the 50 lowest energy conformations obtained in the former step, and further structural optimizations were performed at the B3LYP DFT level complemented by the Grimme's vdW correction (D3) with a 6-311++G(d,p) basis set as implemented in the Gaussian 16 package.[25] We have already assessed the reliability of the DFT (B3LYP(-D3)/6-311++G(d,p)) computational scheme, showing that is able to properly reproduce the relative energies of Ala

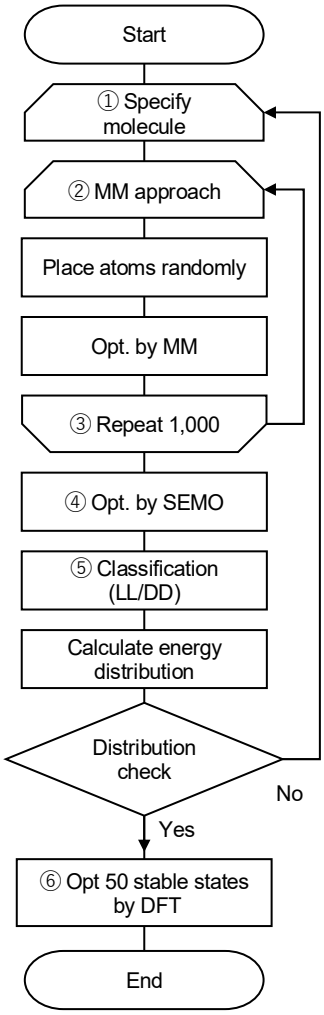

Fig. 1 Flowchart of the random sampling (RS) approach used to search for the amino acids conformers. Three different theoretical levels are used: a classical force field molecular mechanics method (MM), a semi-empirical molecular orbital method (SEMO) and a density functional theory (DFT) scheme. In specific case, additional calculations at the DNPNO-CCSD(T)/ccpvTZ level are done to corroborate the DFT results. The labels LL and DD indicate dimers composed of the same enantiomers and different enantiomers, respectively.

and stable isomers with an accuracy close to CCSD(T)/cc-pVTZ.[23] Moreover, such a DFT approach provided reliable structures for larger size molecules containing intermolecular interactions in active sites of proteins.[26-28] In the present study, DNPNO-CCSD(T)/cc-pVTZ calculations implemented in the ORCA 5.0 package[29] were further carried out to validate the DFT results. The solvation effect of water was incorporated by polarizable continuum model (PCM). In our specific case, the PCM is adapted for the calculation of zwitterion forms. This is essential because amino acids take non-ionic form when not solvated. This PCM also allows to mitigate the computational workload that an explicit treatment of water molecules would imply. The final energies of the dimers are calculated including the zero-point vibrational energy correction. Then, the most stable conformations for each LL and LD were determined for the amino acid dimers.

3 Results

The conformational sampling of the three types of dimers, Ala-Ala, Iva-Iva and Ala-Iva, in the zwitterion form were done in aqueous solution by using the RS method. We confirmed the convergence of the conformational sampling by monitoring whether or not a substantial number of replicas for the stable conformers was realized. Fig. 2A shows the most stable conformers of Ala-Ala, Iva-Iva and Ala-Iva. In Fig. 2B, the second stable conformers are shown along with relative energies in kcal mol^{-1}. Optimized structures of the third stable conformers are shown in the ESI (Fig.S1). Relative energies of all these stable conformers are summarized in Table S1 of the ESI. The LL and LD forms are shown in the upper and lower panels, respectively. In all these conformations, there are two different types of intermolecular interactions; (i) ionic interaction/salt bridge between the carboxy group and the amino group and (ii) H-bond interaction between the hydrogen of the hydrocarbon and the oxygen of carboxy group at least for distances between ~1.6 and ~2.0 Å. For longer distances, weak H-bonds also contribute to molecular interactions, thus to the stability of the structure[21,22]. To get a quantitative analysis of the noncovalent bonds, we used the Bader's Atoms in Molecules (AIM) analysis[30]. The details of this analysis, along with the AIM electron density properties at bond critical points and molecular graphs, are reported in the ESI (Table S2-S4 and Fig. S2).

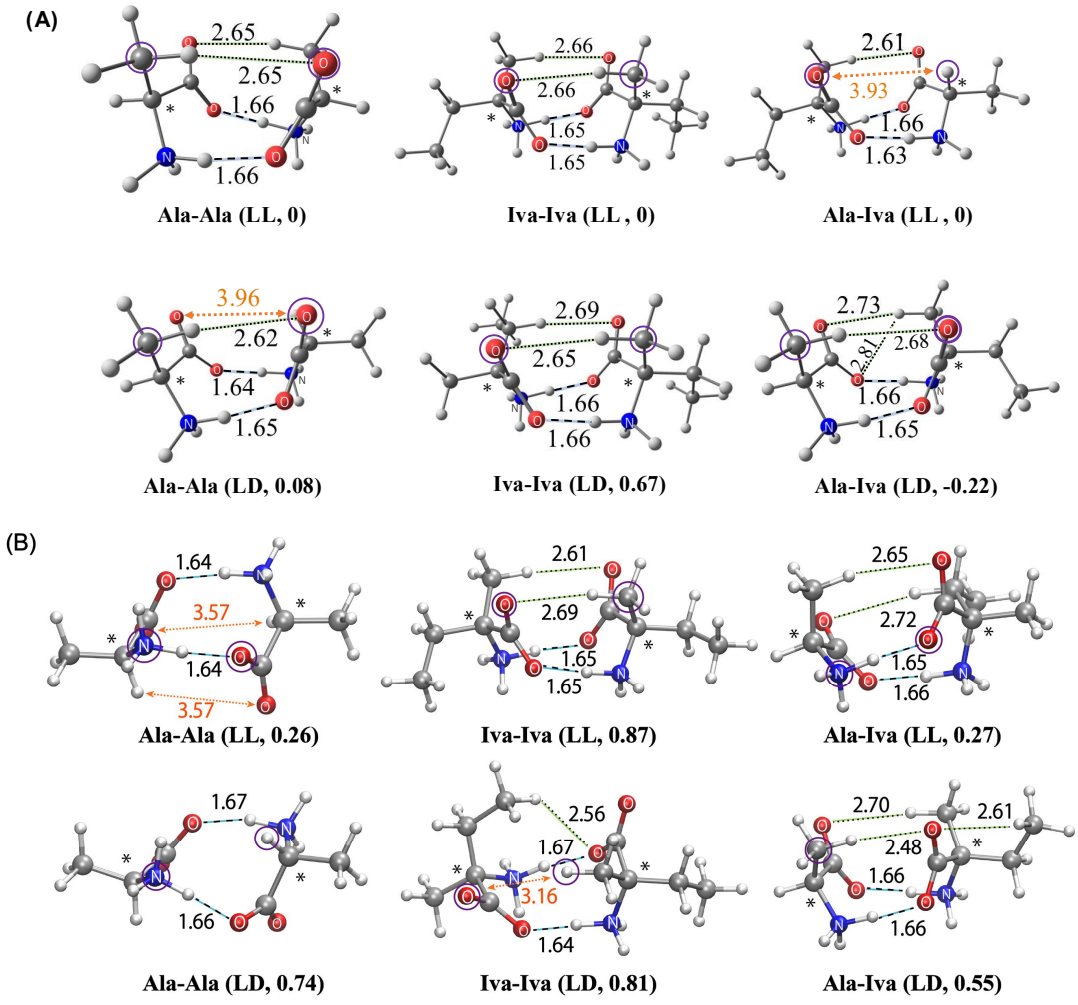

Fig. 2 (A) The most stable conformations of amino acid dimers in the zwitterionic form and (B) the second stable ones. Dashed lines represent the electrostatic ionic interactions, and dotted lines indicate the H-bonds along with their distances in Å. Dotted orange arrows indicate the distances between atoms. Atoms on the front side are evidenced by a circle for clarity. All the conformations are optimized at the B3LYP-D3/6-311++G(d,p) level in PCM. Relative energies (kcal mol^{-1}) to each of the most stable conformations of LL are given in parentheses.

3.1 Ala-Ala

For each of LL and LD form of Ala-Ala, 6,000 conformers were generated including replications. For the most stable conformer of LL, the two Ala units face each other in head to tail orientation by approaching the side chain methyl group, forming two weak H-bonds between the methyl group and the carboxy group, accompanied by two strong ionic interactions. The strength of these interactions results in ionic distances of 1.66 Å, whereas the weak H-bonds result in distances of 2.65 Å. The second stable conformation in Fig. 2B is an orientation realized by approaching the α-H atoms without forming H-bonds, as the atoms are separated by 3.57 Å. On the other hand, for LD, one Ala (left side Ala in Ala-Ala(LD) of Fig. 2A) approaches the methyl group, and the other Ala (right side Ala in Ala-Ala(LD) of Fig. 2A) comes close to the α-hydrogen to form one H-bond. In this case, the distances of the stronger ionic interactions are still comparable to the former case, namely 1.64 and 1.65 Å, and the distance of the H-bond is 2.62 Å. In the second stable conformation in Fig. 2B, all the H-bonds are lost. Among the most stable conformations, LL is more stable than LD by 0.08 kcal mol^{-1}, suggesting that energy difference is not exactly zero, is anyhow rather small and on the verge of the DFT accuracy. These results were corroborated by accurate DLPNO-CCSD(T) calculations, obtaining a small energy difference of 0.17 kcal mol^{-1}, consistent with the DFT result.

3.2 Iva-Iva

For each LL and LD forms of Iva-Iva, more than 100,000 conformers were generated including replicas. The larger sampling reflects their higher conformational freedom. In the most stable LL conformation, the two Iva monomers come close to each other by approaching the α-methyl group, away from their side chain ethyl groups. The distances of the strong ionic interactions turn out to be 1.65 Å, while the distances of the weak H-bonds are both 2.66 Å. The Iva-Iva (LL) conformer is like the one of Ala-Ala (LL) except for the side chains. In the second stable geometry in Fig. 2B, conformations of the side chains are changed. In LD, one Iva (left side Iva in Iva-Iva(LL) of Fig. 2A) brings the methyl group close to the other Iva (right side Iva in Iva-Iva(LL) of Fig. 2A) which, in turn, results in an approaching of the ethyl group close to the former Iva. In this case, the distances realized by the strong ionic interactions are both 1.66 Å, and the distances of the weaker H-bonds are 2.65 and 2.69 Å. In the second stable structure of Iva-Iva(LD) in Fig. 2B, conformations of the side chains change and one H-bond is formed via the ethyl group. Concerning the relative energy difference, LL in the most stable conformations is 0.67 kcal mol^{-1} more stable than LD. This means that Iva dimer is more stable upon aggregation preserving the same chirality. These results were further checked at the DLPNO-CCSD(T) level, obtaining an energy difference of 0.81 kcal mol^{-1} in line with the DFT result. The energy difference of 0.67 kcal mol^{-1} in DFT is substantially large compared with the energy difference of 1.0-1.8 kcal mol^{-1} in the amino acid adsorption on a chiral quartz surface[31] and the 0.24 kcal mol^{-1} in the dimer of propylene oxide[32]. The difference in the dimerization energy can be rationalized by the fact that LL has a certain degree of freedom in the position of the ethyl groups, whereas LD has a restricted space to accommodate one ethyl group involved in the longer H-bond (2.69 Å).

3.3 Ala-Iva

For each of LL and LD forms of Ala-Iva, about 25,000 conformers including replications were considered. In the most stable LL conformer, Ala orients the α-H close to Iva, while Iva brings the α-methyl group toward Ala, forming one weak H-bond with the distance of 2.61 Å. The stronger ionic interactions are, instead, responsible for interatomic distances of 1.63 and 1.66 Å. In the second stable conformation shown in Fig.2B, Ala and Iva come close to each other by approaching their side chains. In LD, both Ala and Iva reorient their methyl groups close to each other to form three weak H-bonds of distances equal to 2.68, 2.73 and 2.81 Å. The stronger ionic interactions result, instead, in distances of 1.65 and 1.66 Å. In the second stable structure, the side chain of Iva changed its conformation and an intramolecular H-bond was formed between the side chain ethyl group and carboxyl oxygen at a distance of 2.61 Å. By looking at the relative energies, we remark that LD in the most stable conformation is more stable by 0.22 kcal mol^{-1} than LL, suggesting that racemic mixture is only slightly preferred by the Ala and Iva interactions.

4 Discussion

The interaction energy (E_{inter}) of each conformation was evaluated by using the supramolecular energy decomposition scheme,[33]

$$E_{inter} = E_{dimer} - \sum_{i=1,2} E_i \quad (1)$$

, where E_{dimer} and E_i are energies of dimer and the energy of each monomer i in the most stable conformation, respectively. The obtained E_{inter} values for Ala and Iva are 17 to 18 kcal mol^{-1}, respectively (Table 1). In the gas phase, E_{inter} of the L-Ala dimer was reported to be -15.62 kcal mol^{-1} at the B3LYP/6-311++G(d,p) level.[20] In the conformation, the carboxy groups are oriented toward each other and only two intermolecular H-bonds are formed. The side chain groups, which are crucial for the molecular chirality, are well separated and away from each other. For a direct comparison, the most stable conformers in the gas phase were recalculated at the identical theoretical level used in the present study in solution. The optimized structures are shown in Fig. 3 and their interaction energies are reported in Table 1. The conformations that form a dimer via their carboxy groups turn out to be unstable in comparison with the zwitterionic conformations by more than 7 kcal mol^{-1} and the relative energy differences between LD and LL are lower than 0.1 kcal mol^{-1} (see Table 1), as expected from the fewer

Table 1. Interaction energies (E_{inter} / kcal mol^{-1}) of the amino acid dimers in zwitterionic and non-ionic forms.[a]

	zwitterion			non-ion		
	Ala-Ala	Iva-Iva	Ala-Iva	Ala-Ala	Iva-Iva	Ala-Iva
LL	-17.20	-18.24	-17.40	-10.11	-9.42	-9.85
	(-14.10)	(-15.08)	(-14.11)	(-8.95)	(-8.54)	(-8.82)
LD	-17.12	-17.57	-17.62	-10.15	-9.42	-9.77
	(-13.93)	(-14.27)	(-14.36)	(-8.98)	(-8.46)	(-8.70)
ΔE_{chir} [b]	–0.08	–0.67	0.22	0.04	0.00	–0.08
	(–0.17)	(–0.81)	(0.25)	(0.03)	(–0.08)	(–0.12)

[a] Calculated at the B3LYP-D3//6-311++G**. Results in parentheses are calculated at DLPNO-CCSD(T)/cc-pVTZ. Zero-point vibrational energy corrections at the B3LYP//6-311++G** are included for all results.

[b] $\Delta E_{chir} = E_{inter}(LL) - E_{inter}(LD)$

number of intermolecular interactions and absence of any interaction to their side chains (Fig. 3).

In all these stable conformations, the strong ionic interactions are kept, and additional weaker H-bonds between methyl group and carboxy group are formed. As the carboxy group can interact with two positively charged atoms, a total of four intermolecular interactions are established in the most stable conformations. We can infer that the enantioselectivity of chiral amino acids arose early, in the dimerization step of crystallization process, and the energy difference in amino acid dimers (ΔE_{chir}), chirodiastaltic energy defined as the energy difference between the homo- and hetero-chiral pair,[31] is a crucial index to rationalize this process. In fact, the relatively large energy difference in Iva-Iva (LL) and small one in Ala-Ala (LL) are consistent with their crystallizations, namely with the fact that Iva forms conglomerate and Ala forms racemic compound.[16] The relative stability of Ala-Iva (LD) indicates that even a high enantiomeric excess of Iva is insufficient to contribute to the ee of Ala, which means the ee are not induced to assume the same racemic type by other amino acids.

Gavezzotti and coworkers reported that the energetic advantage of racemic crystals is not pervasive relative to the homochiral crystals.[34] They inferred that the main reason for the preference of racemic crystals arises just as a consequence of statistical distribution. Conversely, our study shows that a clear (and not statistical) energetic preference exists between the racemic and homo dimers. These results indicate that the energy difference is a dominating feature during the early nucleation stage as in the case of the dimerization studied in this work. Then, the energy difference becomes gradually smaller upon increase of the cluster size. Furthermore, we observe that the structural stability tends to increase with the cluster size. We are not in a position to provide an evaluation of the stabilization energies for larger clusters in the presence of the solvent. However, the stabilized energies in the gas phase per one Ala resulted to be -7.27 and -10.58 kcal mol^{-1} for the dimer and the tetramer, respectively.[20] Nonetheless, these results do not allow for a direct evaluation of free energies during the clusterization. In the more studied case of crystallization of water clusters, stabilization energies per molecule ($\Delta H_n(0\ K)/n$) are -1.6, -3.5, -4.9, -5.3, -6.9 kcal mol^{-1} for dimer, trimer, tetramer, pentamer, and 10-mer, respectively.[35] Their free energy differences per one water molecule in the liquid-ice phase transition ($\Delta G_n(273\ K)/n - \Delta G_1(273\ K)$) turn out to be 0.80, 0.76, 0.25, 0.10, 0.08 kcal mol^{-1} for the same order of multimers.[35] The free energy results for the water clusters suggest that the dimer is the most unstable and is associated to the rate-limiting step in the clusterization process. From this standpoint, we can infer that the molecular properties of the dimers discussed in this study are of fundamental interest for the amino acid crystals. Further investigations, extended to the larger size clusters, closer to the actual crystal packing, and comparisons with other key amino acids such as isoleucine and related isomers would be desirable. We aim at stimulating

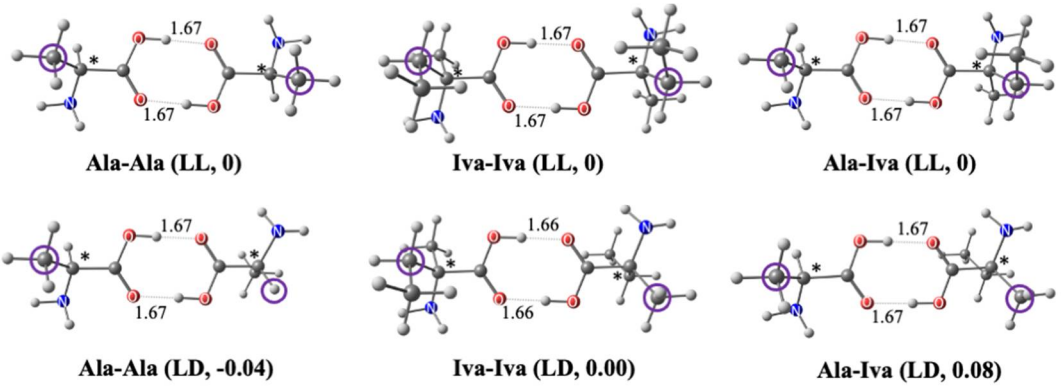

Fig. 3 The structures of amino acid dimers in the non-ionic form. Dotted lines indicate H-bonds along with their atomic distances in Å. Atoms on the front side are highlighted with a circle for clarity. All the conformations are optimized using the B3LYP-D3/6-311++G(d,p) level in PCM. Relative energies (kcal mol^{-1}) for the most stable conformations of LL in the non-ionic form are given in parentheses.

research in this domain in view of some limitations that our RS method still have in handling more than three molecules, due to the fact that the number of geometrical degrees of freedom become excessively large. Improvements of the RS algorithm will be sought in forthcoming work, combined and complemented with computational tools for analyses of cluster growth and isomerization, molecular mechanisms and thermodynamics of the ee of amino acids in meteorites.

5 Conclusion

We focused the present work on the dimerization energy of Ala and Iva in the zwitterionic form by resorting the accurate first principles calculations. The most stable conformers were obtained by the random sampling (RS) method. On these theoretical grounds, we find that the most stable conformations are realized by monomers combining in such a way that the α-methyl group faces the carboxy group of the neighbour molecule, forming tight ionic bonds between carboxyl group and amino group. In Ala-Ala and Iva-Iva, LL dimers are more stable in energy compared to LD dimers. The larger negative chirodiastaltic energies are obtained in Iva-Iva (ΔE_{chir} = –0.67 and –0.81 kcal mol^{-1}) compared to Ala-Ala (ΔE_{chir} = –0.08 and –0.17 kcal mol^{-1}) at both the DFT and DLPNO-CCSD(T) levels. These substantial energy differences of Iva show that Iva has an inherent tendency toward chirality at the stage of dimerization. The small negative chirodiastaltic energies were obtained for the Ala dimers. These results are consistent with the formation of conglomerate crystal in Iva as opposed to the formation of racemic crystal in Ala. Furthermore, we found that dimerized conformers in gas phase are higher in energy than in solution and the dimerization between carboxy groups are expected to give a minor contribution in solution. We can infer that the intermolecular interactions of the Iva dimers in zwitterionic form promote the typical asymmetric interaction between the chiral amino acids, which, in turn, provides an insightful hint into the chiral recognition and enantiomeric discrimination at the molecular level.

Conflicts of interest

The authors declare no conflicts of interest.

Acknowledgements

This research was supported by JST, PRESTO grant number JPMJPR19G6, Japan and JSPS KAKENHI grant numbers 19H00697, 20H05453, 20H05088, JP21H05419, and 22H04916. Computational resources were partially supported by Multidisciplinary Cooperative Research Program in CCS, University of Tsukuba. M.B. thanks the HPC Center at the University of Strasbourg funded by the Equipex Equip@Meso project and the CPER Alsacalcul/Big Data, and the Grand Equipement National de Calcul Intensif (GENCI) under allocation DARI-A0120906092 and A0140906092.

References

1 S. Pizzarello, M. Zolensky and K. A. Truk, *Geochim. Cosmochim. Acta*, 2003, **67**, 1589–1595.
2 D. P. Glavin and J. P. Dworkin, *Proc. Natl. Acad. Sci. USA*, 2009, **106**, 5487–5492.
3 J. M. Friedrich, H. L. McLain, J. P. Dworkin, *et al.*, *Meteorit. Planet. Sci.*, 2019, **54**, 220–228.
4 J. J. Flores, W. A. Bonner and G. A. Massey, *J. Am. Chem. Sci.*, 1977, **99**, 3622-3625.
5 Y. Hori, H. Nakamura, T. Sakawa, *et al.*, *Astrobiology*, 2022, **22**, 1330-1336.
6 A. Sato, M. Shoji, N. Watanabe, *et al.*, Origin of homochirality in amino acids induced by Lya irradiation in the early stage of the Milky way. to be published, 2023.
7 M. Shoji, Y. Kitazawa, A. Sato, *et al.*, J. Phys. Chem. Lett., 2023, **14**, 3243-3248.
8 D. P. Glavin, J. E. Elisa, A. S. Burton, *et al.*, *Meteorit. Planet. Sci.*, 2012, **47**, 1347–1364.
9 D. P. Glavin, J. E. Elsila, H. L. McLain, *et al.*, *Meteorit. Planet. Sci.*, 2021, **56**, 148-173.
10 D. P. Glavin, M. P. Callahan, J. P. Dworkin, J. E. Elsila, *Meteorite. Planet. Sci* 2010, **45**, 1948-1972.
11 J. E. Elsila, D. P. Glavin, J. P. Dworkin, et al., *Proc. Natl. Acad. Sci. USA*, 2012, **109**, E3288.
12 S. Pizzarello, A. A. Monroe, *Proc. Natl. Acad. Sci. USA*, 2012, **109**, E3289.
13 A. S. Burton and E. L. Berger, *Life*, 2018, **8**, 14.
14 C. Viedma, J. E. Ortiz, T. d. Torres, *et al.*, *J. Am. Chem. Soc.*, 2008, **130**, 15274–15275.
15 L. Spix, H. Meekes, R. H. Blaauw, *et al.*, *Cryst. Growth. Des.*, 2012, **12**, 5796–5799.
16 D. P. Glavin, A. S. Burton, J. E. Elsila, *et al.*, *Chem. Rev.*, 2020, **120**, 4660–4689.
17 C. Viedma, C. Lennox, L. A. Cuccia, *et al.*, *Chem. Commun.*, 2020, **56**, 4547‑4550.
18 C. Viedma, P. Cintas, *Isr. J. Chem.*, 2011, **51**, 997-1006.
19 C. Viedma, J. E. Ortiz, T. de Torres, P. Cintas, *Chem. Commun.*, 2012, **48**, 3623-3625.
20 E. J. P. Malar and P. Divya, *J. Phys. Chem. B*, 2018, **122**, 6462–6470.
21 I. V. Fedorova and L. P. Safonova, *Struct. Chem.*, 2021, **32**, 2061-2073.
22 K. Wendler, J. Thar, S. Zahn, B. Kirchner, *J. Phys. Chem. A*, 2010, **114**, 9529-9536.
23 M. Shoji, N. Watanabe, Y. Hori, *et al.*, *Astrobiology*, 2022, **22**, 1129–1142.
24 J. J. P. Stewart, MOPAC2016, Stewart Computational Chemistry, Colorado Springs, CO, USA
25 M. J. Frisch, G. W. Trucks, H. B. Schlegel, *et al.*, Gaussian 16, Revision C.01, Gaussian, Inc., Wallingford CT, 2019.
26 M. Shoji, T. Murakawa, S. Nakanishi, *et al.*, *Chem. Soc.*, 2022, **36**, 10923–10938.
27 M. Hashimoto, K. Miyagawa, M. Singh, *et al.*, *Phys. Chem. Chem. Phys.*, 2023. DOI: 10.1039/d2cp04718g
28 K. Mishima, M. Shoji, Y. Umena, *et al.*, *Bull. Chem. Sci. Jpn.* 2023, DOI:/10.1246/bcsj.20220334.
29 F. Neese, *WIREs Comput. Mol. Sci.*, 2022, **12**, e1606.
30 F. Biegler-König, J. Schönbohm, D. Bayles, *J. Comput. Chem.*, 2001, **22**, 545-559.
31 A. J. Price and E. R. Johnson, *Phys. Chem. Chem. Phys.*, 2020, **22**, 16571–16578.
32 Z. Su, N. Borho, Y. Xu, *J. Am. Chem. Soc.*, 2006, **128**, 17126-17131.
33 K. E. Riley and P. Hobza, *WIREs Comput. Mol. Sci.*, 2011, **1**, 3–17.
34 A. Gavezzotti and S. Rizzato, *J. Org. Chem.,* 2014, **79**, 4809-4816.
35 B. Temelso, K. A. Archer, G. C. Shields, *J. Phys. Chem. A*, 2011, **115**, 12034-12046.

